Ablation of Graphitic Materials in the Sublimation Regime

John H. Lundell* and Robert R. Dickey†
NASA Ames Research Center, Moffett Field, Calif.

A large variety of graphitic materials has been tested in an arc-heated airstream at a surface pressure of 4.3 atm and a nominal surface temperature of 3925 K. Included were commercial and developmental grades of artificial graphites, both two and three-dimensional carbon-carbon composites, and several special materials such as pyrolytic graphite, mesophase graphite, glassy carbon, and natural graphite. ATJ graphite was used as a control material. The mass-loss rate for all the man-made graphitic materials fell within the range of 17% less to 30% more than the rate for ATJ. Thus, it is concluded that wide variations in constituents, processing, fabrication, and structure have relatively little effect on the ablation performance of graphitic materials, at least under the conditions of the present tests. Particulate mass loss was observed for all the materials tested and appears to be the dominant mechanism for mass removal at the present test conditions. It is suggested that this mechanism results from physical failure, primarily by compressive thermal stress.

Nomenclature

C_p = specific heat, cal/g- K
E = elastic modulus, dynes/cm^2
k_c = thermal conductivity, cal/cm-sec- K
k_i = defined by Eq. (2)
$\dot{m}$ = mass-loss rate, g/cm^2-sec
$\dot{m}_{ATJ}$ = mass-loss rate for ATJ graphite, g/cm^2-sec
$\Delta\dot{m}$ = incremental mass-loss rate, g/cm^2-sec
P_{t_2} = pressure at stagnation point, atm
r = radius, cm
R_{n_f} = final nose radius, cm
T_0 = temperature of the unheated specimen, K
T_s = surface temperature, K
V_s = surface recession, velocity, cm/sec
α = thermal expansion coefficient, 1/K
μ = Poisson's ratio
ρ = bulk density, g/cc
σ_t = thermal stress in tangential direction, dynes/cm^2

I. Introduction

GRAPHITIC materials have received much attention in recent years for application to both planetary entry probe heat shields and ballistic missile nose tips and heat shields. To date, however, there is little information in the literature on the ablative behavior of this class of refractory materials in the sublimation regime (above 3500 K). Consequently, an extensive experimental program was initiated to obtain such information. In the initial phase of this work,[1] ATJ graphite was examined extensively in both the diffusion-controlled oxidation regime and the sublimation regime. The objectives were to compare experimental results with the available graphite ablation theories, to ascertain if there are any ablation mechanisms which are not accounted for by the available theories, and to thoroughly characterize ATJ so it could be used as a "control" material in tests of other graphitic materials.

The results of the initial phase of the program demonstrated that particulate mass loss becomes a significant ablation mechanism for ATJ graphite when the surface temperature exceeds about 3600 K. At a temperature of 4000 K, for example, it is estimated that 65% of the mass is lost by particulate removal. As a result, the equilibrium thermochemical ablation theories for graphite[2-5] cannot be used to predict the performance of ATJ graphite in the sublimation regime. These theories simply do not adequately model the ablation process at elevated temperatures.

The question naturally arises as to whether particulate mass loss is significant for other grades of artificial graphite and other types of graphitic materials. Thus, a second phase of the program was initiated to investigate a large variety of graphitic materials in the sublimation regime and to study possible mechanisms for particulate mass loss.

II. Experiments

All the tests were performed in the Ames Heat Transfer Tunnel, which is a conventional arc-driven wind tunnel. The test gas is heated by means of an electric arc heater and then expanded through a supersonic nozzle into an underexpanded free jet. For these tests a Linde N4001 arc heater was coupled to a 5.1 cm diam contoured nozzle with a 1.9 cm diam throat. This combination produces a high-enthalpy air stream with a nominal Mach number of 3.5. A unique feature of the facility is its model support system which contains 18 support arms. Any or all of the support arms can be sequentially inserted into the test stream for a predetermined time by means of an automatic control system.

For the present tests, a standard test condition was selected to produce a high surface temperature and, potentially, a large particulate mass loss. The condition selected was an arc chamber pressure of 21.4 atm, an arc current of 2700 amp, and a nominal voltage of 1830 volts. These conditions resulted in a nominal convective heating rate of 6500 W/cm^2, a centerline enthalpy of 39 Mj/kg, a surface pressure of 4.3 atm, and a surface temperature of about 3925 K. The surface pressure was measured with a copper pitot probe, and the convective heating rate was measured with a transient, slug-type calorimeter which had the same size and shape as the ablation specimen. Surface temperature is a critical measurement which is discussed in some detail in Ref. 1. For the present tests, temperature was measured with an automatic optical pyrometer (Thermodot TD-9), and a surface emissivity of 0.91[6] was used to correct brightness temperature to true temperature.

The test procedure was the same for all the runs. From 10 to 13 ablation specimens were tested during a single run, and in all cases an ATJ graphite specimen was included as a control to account for slight variations in the actual test conditions. Once the specimens and instrumentation were installed, the test chamber was pumped down to a pressure of 200μ, and the arc heater was started and brought to the desired running con-

Presented as Paper 72-298 at the AIAA 7th Thermophysics Conference, San Antonio, Texas, April 10-12, 1972; submitted July 22, 1974; revision received February 24, 1975.

Index categories: Material Ablation; Thermal Stresses.

*Research Scientist, Thermal Protection Branch. Member AIAA.
†Research Scientist, Thermal Protection Branch.

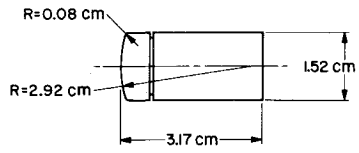

Fig. 1 Ablation specimen.

Table 1 Commercial graphites

Designation	Manufacturer	Filler Type*	Maximum Grain Size mm	Density g/cc	Run Number	R_{bf} cm	T_s K	$\frac{\dot{m}}{\dot{m}_{ATJ}}$
Graph-i-Tite G	Carborundum	PC	.20	1.87	4	4.76	3850	0.97
ME 11**	General Electric	PC, LB, AG	.076	1.63	10	2.79	3945	1.07
ME14**	General Electric	PC, LB, AG	.076	1.74	10	-	-	Broke
ME14**	General Electric				14	2.54	3930	1.04
ME15**	General Electric	LB, PC, AG	.18	1.74	10	2.54	3945	0.93
ME18**	General Electric	PC, LB, AG	.076	1.59	10	2.92	3955	1.10
H-205	Great Lakes Carbon		.41	1.78	4	4.76	3870	1.00
H-205**	Great Lakes Carbon				10	3.43	3945	0.99
H-205-85**	Great Lakes Carbon		.15	1.84	10	3.94	3930	1.02
MHLM**	Great Lakes Carbon	PC	.84	1.78	10	3.18	3945	0.98
MHLM-85**	Great Lakes Carbon	PC	.84	1.86	10	3.68	3955	0.96
2BE**	Ohio Carbon	PC	.15	1.51	11	2.79	3940	1.05
2D8D**	Ohio Carbon	LB	.18	1.48	11	2.03	3905	1.04
2D9B**	Ohio Carbon	LB, PC	.18	1.69	11	1.65	3920	1.23
W11B**	Ohio Carbon	PC, NG	.25	1.74	11	3.68	3920	1.02
AXF-5Q	Poco		.025	1.80	4	5.40	3840	1.20
AXF-5Q	Poco				5	3.68	3910	1.06
AXF-5Q	Poco				8	2.79	3940	1.29
L-56**	Pure Carbon	LB	.15	1.61	11	-	-	Broke
L-56**	Pure Carbon				14	-	-	Broke
L-56(GP)**	Pure Carbon	LB	.15	1.60	11	3.30	3915	1.04
P-03	Pure Carbon		.076	1.82	4	4.76	3840	1.06
P-3W**	Pure Carbon	PC	.15	1.66	11	3.18	3930	0.96
P-3W(GP)**	Pure Carbon	PC	.15	1.64	11	3.18	3930	1.03
3499**	Airco Speer	PC	.076	1.68	12	3.05	3945	1.12
3499S**	Airco Speer	PC	.076	1.59	12	2.92	3945	1.14
39-RL**	Airco Speer	PC	.076	1.63	12	3.05	3930	1.04
4007**	Airco Speer	PC	.20	1.66	12	3.68	3945	1.08
8827**	Airco Speer	PC	.076	1.76	12	3.81	3945	1.08
8882	Airco Speer	PC	.076	1.83	8	2.54	3940	1.21
9050**	Airco Speer	PC	.076	1.78	12	2.92	3940	1.05
9326	Airco Speer	PC	.020	1.90	4	4.45	3890	1.30
9821	Airco Speer		.020	1.92	8	1.78	3935	1.17
9RL**	Airco Speer	PC	.076	1.67	12	3.05	3945	1.11
E-24**	Airco Speer	LB	.13	1.57	12	-	-	Broke
E-24**	Airco Speer				14	-	-	Broke
L1**	Stackpole Carbon	PC	.15	1.64	12	2.92	3955	1.08
L31**	Stackpole Carbon	LB	.15	1.61	12	-	-	Broke
L31**	Stackpole Carbon				14	-	-	Broke
331	Stackpole Carbon	PC	.076	1.70	12	2.79	3935	0.96
2019	Stackpole Carbon			1.82	4	5.40	3805	1.03
AGSX**	Union Carbide	PC	.41	1.64	13	2.67	3945	0.93
ATJ**	Union Carbide	PC	.15	1.73	13	3.30	3945	1.00
ATJ(GP)**	Union Carbide	PC	.15	1.71	13	3.05	3945	0.98
ATJS**	Union Carbide	PC	.15	1.83	13	3.18	3945	0.95
ATJS(GP)**	Union Carbide	PC	.15	1.83	13	3.81	3945	0.92
ATL**	Union Carbide	PC	.76	1.79	13	2.79	3940	0.93
ATL(GP)**	Union Carbide	PC	.76	1.78	13	3.18	3945	0.98
AUC	Union Carbide	PC	.20	1.68	13	2.67	3945	1.17
CDA**	Union Carbide	PC, LB	.15	1.65	13	3.30	3945	0.99
CDG**	Union Carbide	PC, LB	.41	1.50	13	2.92	3945	0.94
CDG(GP)**	Union Carbide	PC, LB	.41	1.49	13	3.18	3945	1.06
CMB**	Union Carbide	PC, LB	.076	1.81	13	3.30	3935	0.94
PGR**	Union Carbide	PC	.76	1.68	13	2.54	3945	0.97
RVA	Union Carbide	PC	.76	1.84	4	3.81	3840	1.15
ZTA	Union Carbide	PC	.15	1.95	4	4.76	3890	0.96

*Filler materials are: AG, artificial graphite; LB, lampblack; NG, natural graphite; PC, petroleum coke.
**Denotes grades investigated by Maahs[7-9]. (GP) denotes a gas-purified version of the standard grade.

dition. The instruments and ablation specimens were then sequentially inserted into the stream for a preselected time, typically 8 sec for the ablation specimens. This exposure time was sufficient to produce a recession of about 0.8 cm for a typical artificial graphite.

The design of the ablation specimen is illustrated in Fig. 1. This shape evolved as a fairly steady-state shape for ATJ graphite during the initial phase of the program. In most cases the specimens were machined so that their centerlines were in the across-grain direction. Exceptions to this procedure will be noted. Since all graphitic materials expand appreciably when heated, a notch was cut in each specimen to provide a "local" reference for the recession measurements. The surface recession history for each specimen was determined by means of motion pictures which were shot at either 24 or 64 frames per sec. The steady-state mass-loss rate was determined by multiplying the recession rate by the bulk density.

III. Materials

A large variety of graphitic materials were investigated in the experimental program. Included were both commercial and developmental grades of artificial graphites, both two- and three-dimensional carbon-carbon composites, and several special materials. In addition, Teflon and boron nitride were included to obtain a direct comparison of graphitic materials with a low-temperature subliming material and another type of refractory material. A total of 85 materials were tested. They are briefly described in Sec. III. in Tables 1-4.

The work on most of the commercial graphites represents a cooperative effort with Dr. Howard Maahs of Langley Research Center. Over a period of several years, he characterized 40 different grades of commercial graphite by examining their chemical impurities,[7] crystallographic structure,[8] and physical microstructure.[9]‡ The selected grades include a wide variety in filler material, grain size, density, impurity level, crystallographic structure, and physical microstructure. Thus, the end objective was to relate these characteristics to the ablative performance[9] of the various grades. The ablation tests performed by Maahs were done in the oxidation regime, at a surface temperature in the range of 2045 K-2300 K. This temperature range is of interest in such applications as the space shuttle, but it is significantly below the range of interest for most planetary probe and ballistic missile applications. Hence, a cooperative effort was initiated, and the same grades were tested in the present program. The commercial graphites obtained from Maahs and those obtained directly from the manufacturer are listed in Table 1.§

In addition to the microstructure, other factors which may influence the ablation behavior of artificial graphites are the initial constituents and the processing of these constituents into the final product. Unfortunately, information regarding these factors is generally not available for commercial graphites; manufacturers treat this as proprietary information. Thus another cooperative effort was initiated with several groups which are working on the development of improved graphites. These groups include the Los Alamos Scientific Laboratory (LASL), Oak Ridge National Laboratory, ORNL, and the McDonnell Douglas Astronautics Company (MDAC).¶

The developmental grades are materials which the several groups thought were representative of their better materials at the time they were supplied. To date there has not been a systematic variation in constituents and processing among the grades investigated. A description of the various developmental grades is given in Table 2, where initial constituents, method of fabrication, and density are listed. In all, 19 grades were received from LASL, two from MDAC, and one from ORNL. The materials from LASL include a variation in filler, addition, binder, crystal orientation, and method of fabrication.[10] The two materials supplied by MDAC provide a variation in type of filler. MDAC 1 is similar to ATJS except that is has filler particles which are half the size of those in ATJS. Thus comparison of these two grades will provide an indication of the effect of particle size on ablation performance. MDAC 228 is made with pyrolytic graphite filler particles to provide a filler which is more anisotropic than that used in MDAC 1. The final developmental grade was IP-59 which was obtained from ORNL. In this material, the filler is low-strength, low-modulus carbon fiber (2μ diam by 250μ long) which is produced in the Y-12 plant at Oak Ridge, and the binder is a coal tar pitch. A description and some thermophysical properties of the IP materials are given in Ref. 11.

It is apparent that the developmental materials provide variations in constituents, fabrication, and processing. Tests on these materials may help to elucidate the effects of filler type and size, binder, additions, calcining temperature, method of molding, and grain orientation on ablation performance.

Carbon-carbon materials are a two-phase system consisting of a graphitic reinforcement in the form of cloth or fiber and a graphitized pitch or resin as the matrix material. They ap-

‡The characterization includes various measures of density; pore radius, area and volume; surface area; porosity; and thermal conductivity. All measurements were performed at room temperature.

§The grades obtained from Maahs are denoted by a double asterisk in Table 1. Several of the grades were obtained in a purified form. Purification was accomplished by high-temperature halogenation (presumably chlorine) of the standard grade. The purified grades are denoted with (GP) after the grade designation.

¶The authors wish to acknowledge the cooperation of M. Smith of LASL, K. Kratsch of MDAC, and W. McWhorter of ONRL in supplying developmental grades for this phase of the program.

Table 2 Developmental graphites

Designation	Supplier	Filler	Filler Fraction	Calcining Temperature °C	Addition	Addition Fraction	Binder	Binder Fraction	Fabrication Method	Orientation	Density g/cc	Run Number	R_{n_f} cm	T_s K	$\frac{\dot{m}}{\dot{m}_{ATJ}}$
65B	LASL	Isotropic Coke	.769	1090			30 MH Pitch	.231	Molded Billet	AG	1.755	6	3.05	3910	1.12
73C	LASL	Isotropic Coke	.794	1090			30 MH Pitch	.206	Molded Billet	AG	1.765	6	3.68	3910	1.19
73F	LASL	Isotropic Coke	.806	2170			30 MH Pitch	.194	Molded Billet	AG	1.799	6	2.79	3895	0.98
77J	LASL	Isotropic Coke	.680	2500	Carbon Black	.120	PFA Resin	.200	Extruded		1.896	7	-	-	Broke
77F	LASL	Needle Coke	.758	1190			30 MH Pitch	.242	Molded to Shape	AG	1.752	7	3.56	3940	1.17
77G	LASL	Needle Coke	.827	2420			30 MH Pitch	.173	Molded to Shape	AG	1.904	7	3.56	3940	1.10
77L	LASL	Needle Coke	.714	2520	Kynol Fiber	.033	30 MH Pitch	.174	Molded to Shape	AG	1.883	7	2.92	3950	1.17
		Fine Natural Graphite	.079												
75K	LASL	Needle Coke	.714	2520	Kynol Fiber	.033	30 MH Pitch	.174	Molded Billet	AG	1.890	6	4.45	3930	1.10
		Fine Natural Graphite	.079												
75K	LASL	Needle Coke	.714	2520	Kynol Fiber	.033	30 MH Pitch	.174	Molded Billet	WG	1.890	6	-	-	Broke
		Fine Natural Graphite	.079												
77B	LASL	Fine Natural Graphite	.814		Kynol Fiber	.034	30 MH Pitch	.152	Molded to Shape	AG	1.817	7	3.18	3930	1.12
75A	LASL	Fine Natural Graphite	.814		Kynol Fiber	.034	30 MH Pitch	.152	Molded Billet	AG	1.908	6	3.56	3915	1.12
77D	LASL	Fine Natural Graphite	.697		Carbon Black	.123	30 MH Pitch	.180	Molded to Shape	AG	1.850	7	2.67	3940	1.00
59K	LASL	Fine Natural Graphite	.697		Carbon Black	.123	30 MH Pitch	.180	Molded Billet	AG	1.819	6	2.79	3910	1.11
59K	LASL	Fine Natural Graphite	.697		Carbon Black	.123	30 MH Pitch	.180	Molded Billet	WG	1.819	6	-	-	Broke
77A	LASL	Coarse Natural Graphite	.842		Kynol Fiber	.035	30 MH Pitch	.123	Molded to Shape	AG	1.930	6	4.19	3910	1.08
77C	LASL	Coarse Natural Graphite	.658		Carbon Black	.219	30 MH Pitch	.123	Molded to Shape	AG	1.865	7	2.92	3930	1.01
75D	LASL	Coarse Natural Graphite	.658		Carbon Black	.219	30 MH Pitch	.123	Molded Billet	AG	1.854	6	3.81	3910	1.07
77E	LASL	Coarse Natural Graphite	.618		Kynol Fiber	.035	30 MH Pitch	.130	Molded to Shape	AG	1.840	7	6.67	3940	1.08
					Carbon Black	.217									
75H	LASL	Coarse Natural Graphite	.618		Kynol Fiber	.035	30 MH Pitch	.130	Molded Billet	AG	1.834	6	3.81	3910	1.09
					Carbon Black	.217									
MDAC 1	McDonnel Douglas	Coke					Pitch	-	Molded Billet	AG	1.850	8	2.79	3945	1.00
MDAC228	McDonnel Douglas	Pyrolytic Graphite	.650				Pitch	.350	Molded Billet	AG	1.849	8	3.18	3940	1.00
IP-59	ORNL	Graphite Fiber					Pitch		Molded Billet		1.85	7	3.30	3945	1.12

Table 3 Carbon-carbon deposits

Designation	Supplier	Description	Reinforcement Type	Reinforcement Fraction	Matrix Type	Matrix Fraction	Addition Type	Addition Fraction	Density g/cc	Run Number	R_{n_f} cm	T_s K	$\frac{\dot{m}}{\dot{m}_{ATJ}}$
AGCarb101	S. R.	Two-dimensional plies parallel to stream	WCA Cloth	.65	Phenolic	.35			1.40	5	3.18	3900	0.92
AGCarb101	S. R.	Two-dimensional plies perpendicular to stream	WCA Cloth	.65	Phenolic	.35			1.40	5	4.76	3900	1.00
3D C/C	MDAC	Three dimensional, coarse weave x-y-z Spacing = .127 x .127 x .318 cm	Thornel 50S		Pitch				1.70	8	1.91	3945	1.02
3D C/C	MDAC	Three-dimensional, fine weave x-y-z-spacing = .094 x .094 x .127 cm	Thornel 50S		Pitch				1.82	8	2.16	3940	1.02

pear to offer great potential as heat shield materials, both from the standpoint of fabricating large pieces and the ability to vary properties in three dimensions. Thus both two-and three-dimensional composites were included to see how their ablation performance compares with artificial graphite. Pertinent information about the structure of the composite materials is given in Table 3. The two-dimensional materials were formulated by San Rafael Plastics Co.,** and the three-

**The authors wish to acknowledge the cooperation of P. Bayliss in furnishing the two-dimensional materials and K. Kratsch in furnishing the three-dimensional materials.

Table 4 Special materials

Designation	Supplier	Processing	Density	Run Number	R_{n_f} cm	T_s K	$\frac{\dot{m}}{\dot{m}_{ATJ}}$
Pyrolytic Graphite	Pfitzer	Pyrolytic Deposition	2.15	8	3.94	4300	0.83
	Pfitzer			14	5.08	4300	1.04
Pyrolytic Graphite	UCAR	Pyrolytic Deposition	2.20	9	4.32	4290	1.04
				14	3.81	4290	1.12
Mesophase Graphite	Great Lakes Res. Lab.		1.813	8	3.43	3945	1.05
Glassy Carbon	Lockheed	Pyrolysis	1.45	15	2.03	3995	1.27
Natural Graphite	Mexico	Mined	1.90	14	0.89	-	8.8
Moldable Graphite	S. R.	Cured	1.69	5	2.03	3900	1.32
Moldable Graphite	S. R.	Pyrolyzed and Graphitized	1.70	5	3.30	3900	1.04
Teflon	Saunders		2.17	9	0.89	-	3.64
Boron Nitride HD0092	Union Carbide	Hot Pressed	1.90	10	1.27		2.09

Table 5 Test conditions and results for ATJ and ATJS

Run Number	Current amp	Chamber Pressure atm	Stagnation Pressure atm	$\dot{m}$ g/cm^2 sec ATJ	$\frac{\dot{m}}{.153}$ ATJ	$\frac{\dot{m}}{.151}$ ATJ	T_s K ATJ	$\dot{m}$ ATJS	$\frac{\dot{m}}{.163}$ ATJS	$\frac{\dot{m}}{.159}$ ATJS	T_s K ATJS
1	2700	21.4		.156		1.03	3925				
2	2700	21.4		.141		.934	3940				
3	2700	21.4	4.13	.153		1.01	3965	.166	1.02	1.04	3965
								.166	1.02	1.04	3965
								.164	1.01	1.03	3965
								.166	1.02	1.04	3965
								.162	.994	1.02	3965
								.154	.945	.969	3965
	Average for Run 3							.163			
4	2700	21.4	4.30	.117			3820	.108			3810
5	2700	21.8	4.33	.144		.954	3930				
6	2700	21.8	4.28	.146		.967	3915				
7	2700	21.4	4.39	.144		.954	3945				
8	2700	21.4	4.40	.144		.954	3940				
9	2700	21.4	4.21	.156	1.02	1.03	3940	.155		.976	3940
				.146	.954	.967	3935				
				.156	1.02	1.03	3935				
				.150	.980	.993	3935				
				.154	1.01	1.02	3935				
				.153	1.00	1.01	3935				
				.153	1.00	1.01	3935				
	Average for Run 9			.153							
10	2700	22.1	-	.164		1.09	3945	.164		1.03	3945
11	2700	21.4	4.47	.154		1.02	3940	.147		.925	3940
12	2700	21.4	4.40	.145		.960	3945				
13	2700	21.4	4.39	.158		1.05		.150		.943	
14	2700	21.4	4.31	.151		1.00	3930				
15	2700	21.4	-	.143		.947	3925				
	Average for All Runs			.151				.159			

dimensional materials were furnished by MDAC.[12] The two-dimensional composites are designated AGCarb 101 since they are one of the materials produced for Aerojet General Corp. for rocket nozzle applications. The materials were made with WCA graphite cloth (Union Carbide Corp.) as the reinforcement and a phenolic resin as the matrix.

The three-dimensional composites differ from each other only in the fineness of weave of the reinforcement. Both materials consist of a three-dimensional, orthogonal structure†† woven with Thornell 50S high-modulus graphite fiber (Union Carbide Corp.) and a proprietary pitch matrix.

A variety of special materials were included in the program to obtain a direct comparison of their ablation performance with both artificial graphites and composites. This group of materials is described in Table 4 and includes pyrolytic graphite, mesophase graphite, glassy carbon, natural graphite, and moldable graphite. One reason the first three of these materials are of interest is that they are single phase rather than two-phase materials such as artificial graphites. It has been suggested[3] that the cause of particulate mass loss in artificial graphites is preferential erosion of the binder phase over the filler phase. If this is indeed the case, the single phase materials should not be susceptible to particulate mass loss.

From the previous brief descriptions of the various materials, it is apparent that they differ significantly in such characteristics as initial constituents, processing, fabrication, and resultant microstructure. The experimental results will now be examined to determine if the variations in these characteristics cause appreciable differences in ablation performance.

IV. Results and Discussion

Experimental results for the four groups of materials are given in the last three columns of Tables 1-4. Included are the final steady-state nose radius (R_{nf}), surface temperature (T_s), and the ratio of the mass-loss rate to the rate for ATJ ($\dot{m}/\dot{m}_{ATJ}$). Generally the materials were tested in groups of 10 to 13, including ATJ as the control, during a single run. In all, 15 runs were made, and the test conditions and ablation results for ATJ for each run are given in Table 5. Note that in Tables 1-4 the number of the run, during which each material was tested, is listed. Thus if the mass-loss rate for any given material is of interest, it may be obtained by multiplying $\dot{m}/\dot{m}_{ATJ}$ by $\dot{m}_{ATJ}$ for the appropriate run.

A. Repeatability

Since a number of runs were required to test all the materials, the question of arc-jet repeatability, from run to run, arises. To account for arc-jet variations, ATJ was used as a control. But what of the repeatability of ATJ? The question of both material and arc-jet repeatability can be answered by examining the results presented in Table. 5.

††Produced by Fiber Materials, Inc.

A check on run-to-run repeatability can be obtained from the results for ATJ for all 15 runs. The results indicate that generally the run-to-run repeatability is within 5%. The major exception to this is run 10, for which the mass-loss rate is 9% above the average. Note, however, that the chamber pressure was somewhat high for this run. The results for run 4 were not included in the average, since the mass-loss rate for this run was exceptionally low. The arc electrodes were reaching the end of their useful life during this run and were replaced, along with the nozzle, after this run. With the exception of run 4, it appears that the run-to-run repeatability may be as high as 9%, but generally it is within 5%.

To check on material repeatability, a separate run (number 9) was made in which seven ATJ specimens were tested. The results show that for all except one specimen, the material repeats within 2%. The exceptional specimen had a mass-loss rate which was 5% below the average for all specimens. Thus it appears that the control material can be expected to repeat within 5%, and probably within 2%. Similar results were obtained on ATJS in run 3, where 6 specimens were tested. In the ensuing discussion, the results are presented relative to the control material, ATJ.

B. Commercial Graphites

The results for the commercial graphites are given in Table 1.‡‡ The first conclusion that is immediately apparent is that no commercial grade has an appreciably lower mass-loss rate than ATJ; the best grade is the gas-purified version of ATJS which has a rate only 8% lower than ATJ. On the other hand, no grade has a significantly higher rate than ATJ. Speer 9326 had the highest rate, but it was only 30% higher than ATJ. Except for the grades tested during run 4, there is very little variation in surface temperature. There is some variation in nose radius, but no correlation with mass loss or material characteristics can be established.

The low percentage variation in mass-loss rate is in contrast to the results of Maahs[9]§§ who found a ratio of 2.8 between his highest and lowest rates. Also the grades with the highest and lowest rates in his tests were not the same as those in the present tests. In fact, there is no correlation in mass-loss results between the two test programs. This fact is not surprising. Maahs' tests were performed in the oxidation regime and show evidence of sizable effects of chemical kinetics; the present tests were performed in the sublimation regime where particulate mass loss is a significant ablation mechanism.

Attempts to relate the mass-loss results to the other microstructural characteristics[9] were not successful. This was also generally true when Maahs[9] attempted to correlate his mass-loss results with the same properties. He did find a trend of increasing mass loss with grain size, but even this trend did not show up in the present results. Either the room temperature values of these properties are not the right values to use, or the set of properties is not complete. The set does not include, for example, some of the thermal and physical properties which influence thermal stress. The possibility of thermal stress failure will be discussed in Sec. IVF.

Particulate mass loss was observed for all the commercial grades tested. The visibility of his phenomenon is related to grain size; it is very difficult to see for very fine grain materials such as AXF-5Q and very readily observed for coarse gain grades such as MHLM. We cannot conclude from this observation, however, that AXF-5Q has a lower mass-loss rate. Quite the contrary, the rate for AXF-5Q is as much as 29% greater than that for ATJ, while MHLM has a 2% lower rate than ATJ.

Summarizing the results for the commercial grades, we find (except for the grades that fractured during the test) a relatively small variation in mass-loss rate for a group of

‡‡Several grades failed during their first test and were retested during later runs.

§§Maahs' tests were performed on 1.27 cm diam hemisphere-cylinder specimens in an airstream at a stagnation pressure of 5.6 atm. The surface temperature varied from 2045 K to 2300 K.

almost 50 grades which differ widely in density, filler material, crystallographic structure, impurities, and physical microstructure. We also find that particulate loss is a significant ablation mechanism for all the grades tested.

C. Developmental Grades

Test results for the developmental grades are given in Table 2, along with the description of the various grades. Again it is obvious that there is not much difference from the performance of ATJ. On a mass-loss basis, the best material (73F) is only 2% better than ATJ, and the worst material (73C) has a 19% higher rate than ATJ. As with the commercial grades, there is very little variation in surface temperature and relatively little variation in nose radius.

Both the grades furnished by MDAC performed as well as ATJ. This is not too surprising in the case of MDAC 1, since it is quite similar to ATJS. As mentioned previously, the major difference between the two grades is in the size of the filler particles, MDAC 1 having particles about half the size of those in ATJS. The smaller particles may improve performance slightly since MDAC 1 performs as well as ATJ, and, on the average, ATJS has a 5% higher mass-loss rate than ATJ, (see Table 5). Since MDAC 228 performs no better than ATJ, we can conclude that there is no advantage to using pyrolytic graphite as a filler material.

The IP-59 material has a 12% higher mass-loss rate than ATJ. Thus carbon fibers do not offer any advantage as a filler material at the present test conditions. As with the commercial grades, particulate mass loss was observed for all the developmental grades.

In summary, the results for the developmental graphites show that a wide variation in initial constituents, processing, and method of fabrication produces a relatively small variation in the performance of artificial graphites. Let us now examine the results for materials which are significantly different in structure.

D. Carbon-Carbon Composites

The experimental results for both the two-and three-dimensional composite materials are given in Table 3. The two-dimensional material was tested with the fabric plies oriented both parallel and perpendicular to the airstream. Surprisingly the material performs better with the plies in the parallel direction. In this orientation the material had an 8% lower mass-loss rate than ATJ, while in the perpendicular orientation its rate is identical to that of ATJ. Both three-dimensional composites performed about as well as ATJ. Thus, it appears that the fineness of weave of the reinforcing fiber has no effect on performance, at least at the present test condition.

Results for the composite materials are both encouraging and discouraging. They are encouraging from the standpoint that both types perform as well as artificial graphite and yet offer much greater flexibility of fabrication. On the other hand, the results are discouraging because even with high-strength, high-modulus graphite fiber as the reinforcement, composite materials do not perform significantly better than artificial graphite. As with the artificial graphites, particulate mass loss was observed during the tests of all the composite materials. Thus marked changes in the structure of graphitic materials do not alleviate this problem.

E. Special Materials

The results for the last group of materials, the special materials, are presented in Table 4. This group includes the single phase materials, natural graphite, and the moldable materials.

On the whole, the single-phase materials have a somewhat higher mass-loss rate than ATJ. The Pfizer pyrolytic graphite did perform about 17% better than ATJ during its first test and thus had the lowest mass-loss rate of all the materials tested. But its performance proved to be erratic; during a second test it had a rate of 4% higher than ATJ. The other grade of pyrolytic graphite (Union Carbide) was also erratic; its mass-loss rate varied from 4%-12% higher than ATJ. Particulate mass loss was observed for these materials, but gross failure by delamination was not a problem. The mesophase graphite has a value of $\dot{m}$ which is 5% higher than that for ATJ. It too produced a shower of particles. The poorest performer of the single phase materials was glassy carbon which had a 27% higher mass-loss rate than ATJ. This may result because this material is not fully graphitized. Very fine particles were visible in the downstream flow while the glassy carbon was being tested, and the specimen finally shattered when it got very thin at the stagnation point.

The Mexican natural graphite had, by far, the highest ablation rate of all the materials investigated. It ablated at 8.8 times the rate of ATJ, and produced a profuse shower of both liquid and solid particles.

The moldable materials had measurably different performance. The material which has just been cured had a 32% higher mass-loss rate than ATJ, while the material which has been pyrolyzed, graphitized, impregnated and then regraphitized performed about as well as ATJ.

For comparison purposes, the results for Teflon and boron nitride are also included in Table 4. Teflon, which sublimes under the present test conditions, ablated 3.6 times as fast as ATJ. Boron nitride, which is sometimes called white graphite because of the similarity of its crystal structure to that of graphite, ablated at twice the rate of ATJ.

In concluding Sec. IVE, it should be noted that particulate mass loss appears to be significant ablation mechanism for all graphitic materials at a temperature close to 4000 K. The results for the single phase materials provide an interesting insight into the problem. The most prevalent theory for particulate removal[3] is that intrinsic differences between the two or more phases in a graphite result in the preferential recession of the binder over the filler. This leaves the filler particles unsupported and susceptible to removal by aerodynamic forces. We can conclude from the present results on the single phase materials, however, that preferential recession is not the complete answer, for by this model the single phase materials should not exhibit particulate mass loss. Thus there must be other causes for this phenomenon. One possibility is that the materials simply fail physically; that is, they have inadequate high-temperature strength properties.

F. Thermal Stress

Howe[13] has considered the problem of thermal stress in an ablating elastic material exposed to uniform electromagnetic radiation. One special case which he treats is that where all the radiation is absorbed at the surface and conducted inward. This case can be applied to convective heating if the input heating is assumed to be the hot-wall convective heating rate diminished by the effects of convective blockage and reradiation. At the surface, the radial stress is zero, and the tangential stress is compressive. The compressive stress is maximum at the surface, and for a solid hemisphere is given by

$$\sigma_t(r) = -\frac{\alpha E}{1-\mu}\left\{1-\frac{3}{k_i r}\left[1-\frac{2}{k_i r}+\frac{2}{(k_i r)^2}-\frac{2}{(k_i r)^2}e^{-k_i r}\right]\right\}(T_s-T_0) \tag{1}$$

where the negative skin indicates a compressive stress, r is the radius, and

$$k_i = \rho V_s c_p / k_c = \dot{m} c_p / k_c \tag{2}$$

Note that the thermal stress is coupled to the ablation rate through the k_i term. The significance of this coupling will be

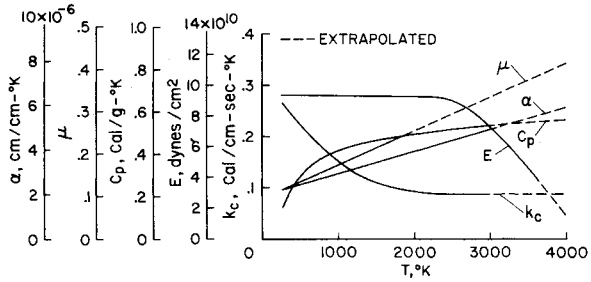

Fig. 2 Thermophysical properties for ATJ graphite.

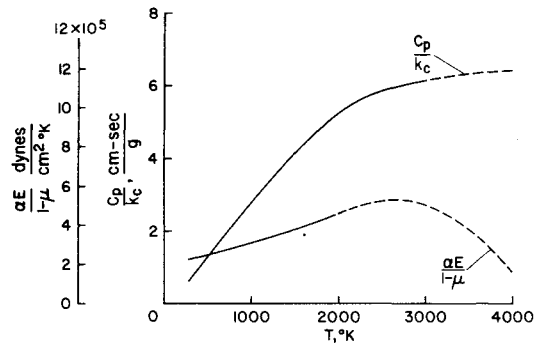

Fig. 3 Significant combinations of thermophysical properties for ATJ graphite.

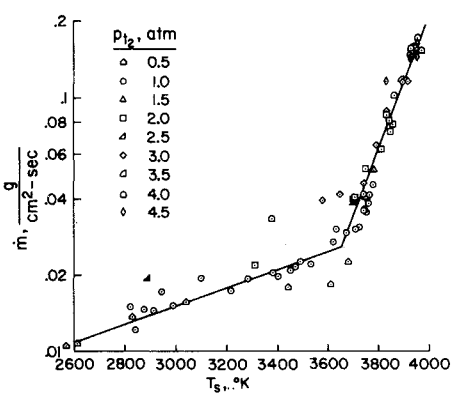

Fig. 4 Mass-loss rate for ATJ graphite.

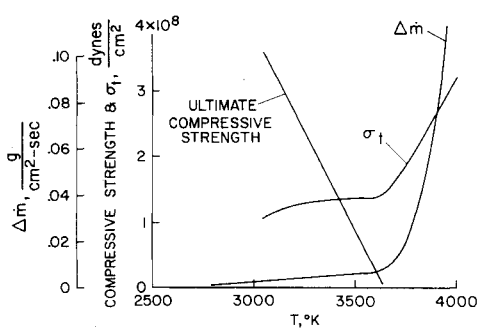

Fig. 5 Comparison for thermal stress, compressive strength and incremental mass-loss rate for ATJ graphite.

discussed later. For simplicity, let us rewrite Eq. (1) in the form

$$\sigma_t(r) = -\frac{\alpha E}{1-\mu}\,[1-f(k_i r)]\,(T_s - T_0) \qquad (3)$$

which contains three terms; $\alpha E/1-\mu$ which involves only thermophysical properties, $f(k_i r)$ which involves the geometry, the ablation rate, and two thermal properties, and lastly a temperature difference term.

To obtain this simple closed-form solution, it is necessary to assume that the ablation process is steady state and that the material properties are independent of temperature. This latter assumption is not very realistic for graphitic materials, because all graphite properties vary with temperature. Note, however, that there are compensating effects; the thermal expansion coefficient α and Poisson's ratio μ increase with temperature, while the elastic modulus E decreases. As will be indicated later, the compensations are not perfect, at least for ATJ graphite. In the k_i term, both the specific heat c_p and thermal conductivity k_c become fairly insensitive to temperature above 2500 K.

Even though graphite properties do vary with temperature, Eq. (3) can be applied to ATJ graphite to obtain a first-order estimate of thermal stress for the conditions of the present tests.¶¶ To obtain such an estimate, properties values to 4000 K must be available. No data exist to that temperature level as can be seen in Fig. 2 where the available necessary data are compiled. Some of the properties shown are sensitive to crystallite orientation; for these properties, values for the with-grain direction were selected. For most of the properties, the extrapolation shown on the figure is not extensive and takes place after the trend with temperature is well established. The properties shown in Fig. 2 were compiled from Refs. 14-17.

The properties have been combined into appropriate groups, as suggested by Eqs. (1) and (2), and plotted in Fig. 3. Here it is evident that the compensating effects mentioned earlier are not perfect. The group $\alpha E/1-\mu$ varies by a factor of 3, while c_p/k_c is fairly constant in the high-temperature range.

Now let us consider the k_i term which involves the mass-loss rate. The available mass-loss data on ATJ from both the previous work[1]*** and the present investigation are plotted against surface temperature in Fig. 4. At lower temperatures the mass-loss rate varies with pressure, but at higher temperatures (where particulate mass loss is the dominant ablation mechanism) the data correlate reasonably well with temperature. For purposes of the present approximate analysis, the mass loss variation with temperature represented by the solid curve will be used. Based on this approximation, and the fact that ratio c_p/k_c depends solely on temperature, it is apparent that k_i is a function of temperature alone.

From the previous discussion, we see that all the terms in Eq. (3) for σ_t are functions of temperature, and thus, to a first approximation, σ_t depends solely upon temperature. This functional relationship is plotted in Fig. 5.

G. Particulate Mass Loss

The possibility that thermal stress is the cause of particulate mass loss can now be investigated by comparing the calculated stress with the ultimate compressive strength of ATJ graphite.[18] Such a comparison is made in Fig. 5 where we see that the compressive strength decreases with increasing temperature, and that failure is predicted at about 3500 K. Note that as temperature increases above the failure value, the thermal stress increases very rapidly. This, of course, is a result of the coupling between stress and the mass-loss rate, Eqs. (1) and (2), and the fact that the mass-loss rate increases rapidly in this temperature range (Fig. 4). It appears that at temperatures above 3500 K, the material is heated to a point above which its physical integrity can be maintained. As temperature increases, thermal stress increases, causing an increase in particulate mass loss. Thus the total mass-loss rate (thermochemical plus particulate) increases, which, in turn, increases the stress and so on until a steady-state condition is established.

The sharp increase in the experimental mass-loss rate at about 3600 K is an experimental result which is not predicted

¶¶Since the ablation specimen is not hemispherical, the actual nose radius of the unablated specimen is used.

***Only earlier data obtained with the ablation specimen shown in Fig. 1 are used in the analysis.

by thermochemical ablation theory. This fact is readily shown by the correlation[1] of the incremental mass-loss rate (the difference between the experimental and theoretical mass-loss rates) with temperature. This correlation is reproduced in Fig. 5 as the curve labeled $\Delta\dot{m}$. From this curve it is apparent that the experimental results are in reasonable agreement with the theory until the surface temperature exceeds the failure temperature. Above this temperature, however, the experimental mass-loss rate increases much more rapidly than the theoretical rate. This effect is the result of particulate mass loss which begins to appear at temperatures above 3000 K but becomes dramatically more visible at temperatures above 3600-3700 K. The presence of particulate mass loss at lower temperatures is probably the result of preferential thermochemical ablation of the binder phase over the filler phase in the ATJ graphite. At higher temperatures, however, the present analysis suggests the particulate mass loss is the result of thermal stress as well as preferential ablation. In fact, preferential ablation will weaken the surface material and make it more susceptible to physical failure.

Although the previous analysis has been specialized to ATJ, it is believed to be qualitatively applicable to all graphites. The high temperature properties that have been measured on other grades show trends similar to those of ATJ. The temperature at which the compressive strength approaches zero may vary, and thus there will be some variation in the temperature at which particulate mass loss begins to dominate the ablation process. The results of the present tests indicate, however, that this temperature is below 4000 K for all the artificial graphites and other graphitic materials tested. This poses a serious problem in the application of graphitic materials to probes entering the atmospheres of the large outer planets. An analysis of Jovian entry probes[19] indicates that the surface temperature of a graphite heat shield may reach 4500 K.

V. Summary and Conclusions

An experimental investigation has been conducted on 85 different graphitic materials in an arc-heated wind tunnel at a surface pressure of 4.3 atm and a nominal surface temperature of 3925 K. The principal objectives were to determine if there are significant differences in the ablative behavior of graphitic materials which have grossly different physical structure and to see if particulate mass loss is an important ablation mechanism for all such materials. Included were commercial and developmental grades of artificial graphite, both two and three-dimensional carbon-carbon composites, and special materials such as pyrolytic graphite, mesophase graphite, glassy carbon, and natural graphite. For control purposes, ATJ graphite was included in each run.

The experimental results can be summarized as follows: 1) The mass-loss rate $\dot{m}$ of the control material, ATJ, repeats within at least 5%, and generally within 2%. 2) For the artificial graphites, $\dot{m}$ varied from 8% below to 30% above the rate for ATJ. 3) The composite materials had values of $\dot{m}$ that varied from 8% below to 2% above the value for ATJ. 4) In general, the single-phase materials (pyrolytic graphite, mesophase graphite, and glassy carbon) had values of $\dot{m}$ greater than that for ATJ. 5) Particulate mass loss was observed for all the materials tested.

Several conclusions can be drawn from the present study:

1) Wide variations in density, initial constituents, processing, fabrication, and structure have relatively little effect on the ablation performance of graphitic materials, at least at the present test conditions.

2) The mass-loss rate of commercial artificial graphites cannot be correlated with any of the microstructural properties reported in Ref. 9.

3) The observation of particulate mass loss for the single-phase materials indicates that this phenomenon is not solely the result of preferential ablation between different phases.

4) An analysis of the effects of thermal stress indicates that particulate mass loss probably results from physical failure. Particulate mass loss increases with temperature because the compressive stress is coupled to the total mass-loss rate.

5) Apparently none of the materials tested have sufficient strength at a temperature of 4000 K to maintain their physical integrity under ablation conditions. Much work remains to be done on the development of graphitic materials with improved high-temperature properties.

References

[1] Lundell, J. H. and Dickey, R. R., "Ablation of ATJ Graphite at High Temperatures," *AIAA Journal*, Vol. 11, Feb. 1973, pp. 216-222.

[2] Dolton, T. A., Goldstein, H. E., and Maurer, R. E., "Thermodynamic Performance of Carbon in Hyperthermal Environments," *Progress in Astronautics and Aeronautics: Thermal Design Principles of Spacecraft and Entry bodies,* Vol. 21, ed. Jerry T. Bevans, Academic Press, New York.

[3] Kratsch, K. M., Martinez, M. R., Clayton, F. I., Greene, R. B., and Wuerer, J. E., "Graphite Ablation in High Pressure Environments," AIAA Paper 68-1153, Williamsburg, Va., 1968.

[4] Fogaroli, R. P. and Brant, D. N., "Re-Evaluation of Graphite Thermochemical Ablation," Fundamentals Memo TFM-9151-060, Oct. 1968, Thermodynamics Laboratory, Re-entry Systems Dept., General Electric Co., Philadelphia, Pa.

[5] McCuen, P.A., Schaefer, J.W., Lundberg, R.E., and Kendall, R.M., "A Study of Solid Propellant Rocket Motor Exposed Materials Behavior," Final Rept., Contract AF 04(611)-9073, Feb. 26, 1965, Vidya Division, Itek, Corp., Palo Alto, Calif.

[6] Wilson, R. G. and Spitzer, C. R., "Visible and Near-Infrared Emittance of Ablation Chars and Carbon," *AIAA Journal*, Vol. 6, April 1968, pp. 665-671.

[7] Maahs, H. G. and Schryer, D. R., "Chemical Impurity Data on Selected Artificial Graphites with Comments on the Catalytic Effect of Impurities on Oxidation Rate," TN D-4212, Oct. 1967, NASA.

[8] Maahs, H. G., "Crystallographic Data on Selected Artificial Graphites with Comments on the Role of the Degree of Crystal Development in Oxidation," TN D-4888, Nov. 1968, NASA.

[9] Maahs, H. G., "Determination of the Effects of Graphite Material Properties on Ablation Performance," AIAA Paper 72-295, San Antonio, Texas, 1972.

[10] Smith, Morton, C., "CMB-13 Research on Carbon and Graphite, Report No. 18, Summary of Progress from May 1 to July 31, 1971," March 1972, Progress Rept. LA-4896-PR, Los Alamos Scientific Laboratory, Los Alamos, New Mex.

[11] Auerbach, I., Bader, B. E., and McBride, D. D., "Recent Graphite Nosetip Developments," AIAA Paper 71-417, Tullahoma, Tenn., 1971.

[12] Kratsch, K. M., Schutzler, J. C., and Eitman, D. A., "Carbon-Carbon 3-D Orthogonal Material Behavior," AIAA Paper 72-365, San Antonio, Texas, 1972.

[13] Howe, J. R., "Thermal-Mechanical Response of Nearly Opaque Materials Exposed to Continuous Radiation," *AIAA Journal*, Vol. 9, Oct. 1971, pp. 1911-1920.

[14] Anon, "High Temperature Properties of Graphite," Report from Southern Research Institute to Aerospace Corp., July 18, 1966, Birmingham, Ala.

[15] Anon., "UCAR Premium Graphite Grade ATJ," Technical Information Bulletin 463-205, Union Carbide Corp., New York.

[16] Kachur, V., "Properties of ATJ Graphite," Westinghouse Nuclear Laboratory Rept. WANL-TME-956, Nov. 1964, Westinghouse Electric Co., Pittsburgh, Pa.

[17] Anon., "Re-entry Materials Handbook," (Title Unclassified), Rept. TOR-1001 (S2855-20)-3, 1968, Aerospace Corp., El Segundo, Calif.

[18] Janowski, K. R., "Progress Report Number 2 on DM15C Mechanical Properties Evaluation," Rept. MP20230, May 1962, Douglas Aircraft Co., Long Beach, Calif.

[19] Wakefield, R. M. and Lundell, J. H., "Ablative Heat Shields for Jupiter Entry Probes," *Advances in the Astronautical Sciences*, Vol. 29, Part 2, ed. Juris Vagners, American Astronautical Society, Washington, D.C., 1971, pp. 229-251.